Aquatic Toxicology 182 (2017) 91–101

Contents lists available at ScienceDirect

Aquatic Toxicology

journal homepage: www.elsevier.com/locate/aquatox

Research paper

Crude extract of cyanobacteria (*Radiocystis fernandoi*, strain R28) induces liver impairments in fish

M.G. Paulino[a], D. Tavares[a], F. Bieczynski[b], P.G. Pedrão[a], N.E.S. Souza[a], M.M. Sakuragui[a], C.M. Luquet[b], A.P. Terezan[c], J.B. Fernandes[c], A. Giani[d], M.N. Fernandes[a,*]

[a] Department of Physiological Sciences, Federal University of São Carlos, São Carlos, São Paulo, Brazil
[b] Center of Applied Ecology of Neuquen, INIBIOMA, UNCo-CONICET- Ruta Provincial 61, km 3, 8371, Junín de los Andes, Neuquén, Argentina
[c] Department of Chemistry, Federal University of São Carlos, São Carlos, São Paulo, Brazil
[d] Department of Botany, Federal University of Minas Gerais, Belo Horizonte, MG, Brazil

ARTICLE INFO

Article history:
Received 5 September 2016
Received in revised form
12 November 2016
Accepted 15 November 2016
Available online 17 November 2016

Keywords:
Microcystin accumulation
Liver ultrastructure
Muscle
PP1 and PP2A activity
Hoplias malabaricus

ABSTRACT

Radiocystis fernandoi R28 strain is a cyanobacterium which produces mostly the RR and YR microcystin variants (MC-RR and MC-YR, respectively). The effects of crude extract of the *R. fernandoi* strain R28 were evaluated on the protein phosphatases and on the structure and ultrastructure of the liver of the Neotropical fish, *Hoplias malabaricus*, after acute and subchronic exposure. Concomitantly, the accumulation of the majority of MCs was determined in the liver and muscle. The fish were exposed to 120.60 MC-RR+MC-LR kg-fish^{-1} (= 100 μg MC-LReq kg-fish^{-1}) for 12 and 96 h (one single dose, acute exposure) and 30 days (one similar dose every 72 h, subchronic exposure). MCs did not accumulate in the muscle but, in the liver, MC-YR accumulated after acute exposure and MC-RR and MC-YR accumulation occurred after subchronic exposure. Protein phosphatase 2A (PP2A) activity was inhibited only after subchronic exposure. Acute exposure induced liver hyperemia, hemorrhage, changes in hepatocytes and cord-like disorganization. At the ultrastructural level, the decreasing of glycogen and lipid levels, the swelling of mitochondria and whirling of endoplasmic reticulum suggested hepatocyte necrosis. Subchronic exposure resulted in a complete disarrangement of cord-like hepatocytes, some recovery of mitochondria and whirling endoplasmic reticulum and extensive connective tissues containing fibrous materials in the liver parenchyma. Despite microcystin toxicity and liver alterations, no tumor was induced by MCs. In conclusion, the increased algal mass of *R. fernandoi* in tropical freshwater, producing mainly MC-RR and MC-YR variants, results in fish liver impairments.

1. Introduction

Cyanobacteria are important components of phytoplankton in most freshwater ecosystems worldwide and include a large number of toxin-producing species. Among toxins, the microcystins (MCs) are hepatotoxic to animals and humans (Carmichael et al., 2001). Structurally, the MCs are cyclic heptapeptides having a cyclo-(D-alanine 1-X2-D-MeAsp3-Z4-Adda 5-D-glutamate 6-Mdha7), in which the position of 2 and 4 amino acids are variable L-amino acids (Carmichael, 1997). Over 70 MCs variants have been identified, and the MC-LR, which has arginine and leucine as the amino acids in position 2 and 4 respectively, is the most toxic and commonly found (Andrinolo et al., 2008).

The genus *Radiocystis* (Cyanobacteria, Chroococcales) is morphologically similar to *Microcystis* except for a few characteristics, such as radially oriented cell disposition and crosswise cell division in one plane (Pereira et al., 2012). In the last decade, this genus has been reported as one of most abundant in cyanobacterial blooms in tropical freshwater (Sant'Anna et al., 2008). The species, *Radiocystis fernandoi* is abundant in Brazilian freshwater blooms (Borges et al., 2008; Fonseca et al., 2011; Sant'Anna et al., 2008), reaching up to 70% of the total cyanobacterial biomass in some blooms (Borges et al., 2008). According to Vieira et al. (2003), the level of MC-LR production may be elevated in this cyanobacterium species; however, Pereira et al. (2012) showed that numerous *R. fernandoi* strains isolated from different reservoirs in Brazil did not produce MC-LR as majority toxin. Currently, there are little information about *R. fernandoi* and its toxicity for freshwater organism.

* Corresponding author at: Departamento de Ciências Fisiológicas, Universidade Federal de São Carlos, Via Washington Luiz, km 235, 13565-905–São Carlos, SP, Brazil.
E-mail address: dmnf@ufscar.br (M.N. Fernandes).

http://dx.doi.org/10.1016/j.aquatox.2016.11.012
0166-445X/

Fish may be impacted for days or weeks by toxins produced during cyanobacterial blooms and, despite the damages caused by such toxins, they seem to be less susceptible to them than other vertebrates (Zhang et al., 2013). In general, MCs inhibit serine threonine protein phosphatases 1 and 2A (PP1 and PP2A, respectively), which affect cell physiology resulting in hyperphosphorylation of proteins, disruption of the cytoskeleton and other hepatocyte changes (Bieczynski et al., 2014; Falconer and Yeung, 1992; Li et al., 2005).

Numerous cyanobacterial toxicity studies have evaluated fish exposed to one MC variant, particularly MC-LR (Atencio et al., 2009; Bieczynski et al., 2013; Ernst et al., 2006; Fischer et al., 2000; Hao et al., 2008; Li et al., 2005); however, more than one type of MC, along with other algal products are present in aquatic ecosystems during cyanobacterial blooms. Thus, exposure to the crude extract of cyanobacteria represents a more realistic condition than purified MCs (Palíková et al., 2003).

In this context, the aim of the present study was to evaluate the effects of crude extract of *Radiocystis fernandoi* strain R28on structure and function of liver and to examine the potential accumulation of these toxins in the liver and muscle of the fish *Hoplias malabaricus* after acute and subchronic exposure.

2. Materials and methods

2.1. R. fernandoi *strain R28 cyanobacteria cultivation and extract preparation*

R. fernandoi strain R28 was isolated from cyanobacterial blooms in the Furnas reservoir (20°40′S; 46°19′W), located in Minas Gerais State, Brazil. This strain, produces MC-RR and MC-YR and minute amounts of other variants, but does not produce MC-LR (Pereira et al., 2015; Pereira and Giani, 2014; Pereira et al. 2012). *R. fernandoi* was cultivated at 25–30 mol m^{-2} s^{-1} irradiance under a 12 h light:12 h dark photoperiod at 20 °C according to Pereira et al. (2012) in the Phycology Laboratory of Botany Department of Federal University of Minas Gerais. Crude cyanobacterial extract was obtained from freeze-dried cyanobacteria which was homogenized in 10 mL of 80% HPLC-grade methanol (PanReac AppliChen, Castellar del Vallès, Spain) in Milli-Q water (18 M Ω cm^{-1}) (Merck KGaA, Darmstadt, Germany) (v:v) using an Ultra Turrax (IKA – T10). Thereafter, the homogenate was centrifuged at 18514*g* for 20 min at 18 °C (Eppendorf 5810 R, Germany). The supernatants were pooled together and evaporated at room temperature in a vacuum solvent evaporator (SpeedVac®). Dried extract were resuspended in milli-Q water and then the total MC-LR equivalents (MC-LReq) in the extract were quantified using the enzyme-linked immunosorbent assay (ELISA) commercial kit (Beacon Analytical Systems Inc., U.S.) in a Molecular Devices Spectra MAX GEMINI X (Molecular Devices, U.S.) at 450 nm.

2.2. *Microcystins quantification in the extract using HPLC-UV analysis*

Quantitative confirmation of the majority presence of MC-RR and MC-YR was achieved using a reverse-phase high performance liquid chromatography system (HPLC-UV, Agilent 1200 Series, Agilent Technologies, Santa Clara, USA). This system was equipped with a G1322A degasser, a G1311A quaternary pump, a G 1367B auto-sampler, a G 1316A thermostatted column and a G1316A diode array detector according to Aranda-Rodriguez et al. (2005), with minor modifications. The MC concentrations were determined by comparing the peak areas of the test samples with those of standard solutions containing MC-LR, MC-YR and MC-RR (Sigma, USA). The chromatographic separation of MCs was achieved using 15 × 0.46 cm 100 Å (10 μm) and 110 Å (5 μm) C-18 ODS Phenomenex columns with mobile phases of MilliQ water (A) and methanol (B), both acidified with 0.05% formic acid. The applied gradients (A-B%) were 10–30% B (10 min), 30–55% B (15 min), 55–100% B (28 min) and 100% B (7 min), with λ = 240 nm, 1.0 mL min^{-1} flow rate and 20 μL volume injected. MC-RR and MC-YR were identified in the extract and the peak areas of the standard solutions containing MC-LR, MC-YR and MC-RR (Sigma, USA) were applied for quantification of these microcystins.

2.3. *Experimental design*

Juveniles traíra, *H. malabaricus* (n = 60 from both sexes, body mass 260.6 ± 9.44 g; body length 27.5 ± 0.16 cm) was purchased from Santa Candida fish farm (Santa Cruz da Conceição, São Paulo State, Brazil). *H. malabaricus* is a carnivorous fish species widespread throughout South America except for, the West Andes and Patagonian areas, and well appreciated for human consumption (Nakatani et al., 2001). Fish were acclimated for 30 days in 1000-L tanks containing dechlorinated tap water and constant aeration at 25 ± 1 °C. The fish were fed with fish pieces every 72 h according to the natural feeding habits of this species.

The fish were randomly distributed into six groups (n = 10 in each group) in 1000-L tanks. The acute exposure experiments consisted of two control groups (C) and two crude extract groups (CE) which received only one injection (a single dose); one C and CE groups were analyzed 12 h (C12 h; CE12 h) post-injection and, the other C and CE groups were analyzed 96 h (C96 h and CE96 h) post-injection. The subchronic exposure experiments consisted of one C and one CE group, which received one dose i.p. injection every 72 h during 30 days (C30 d and CE30 d). All control groups were injected with 0.5 mL of sterile saline (0.9% NaCl) and the CE groups were injected with *R. fernandoi* crude extract containing 120.60 MC-RR + MC-LR kg^{-1} (= 100 μg MC-LReq kg-$fish^{-1}$) diluted in 0.5 mL of sterile saline. This MC-LReq represents relevant environmental concentration found in Brazilian aquatic systems (Santos and Bracarense, 2008). After each experiment, the fish were anesthetized with benzocaine (0.1 g L^{-1}) and killed by severing the spinal column. The liver was removed and macroscopically analyzed. Liver samples were collected and frozen at −80 °C for biochemical analyses; other liver samples were fixed with aqueous Bouin's fluid for light microscopy (LM) or 2.5% glutaraldehyde solution in 0.1 M phosphate buffer, pH 7.3, for transmission electron microscopy (TEM) analyses. Liver and muscles samples were also collected for MC accumulation analyses.

The University Federal of São Carlos Animal Ethics Committee approved this study (Proc. n.026/2012).

2.4. *HPLC-ESI-MS/MS analyses of MC variants in the liver and muscles*

The MC extraction and tissue sample preparation were performed according to Deblois et al. (2011) and Mekebri et al. (2009), with minor modifications. Fresh liver (50 mg) and muscle (100 mg) tissue samples were homogenized in 10 mL of 80% methanol solution (MeOH:H_2O). The extracts were centrifuged at 18514.08*g* for 20 min at 18 °C, and the supernatants were dried in a vacuum solvent evaporator at room temperature. The extract was re-solubilized in 1 mL of deionized water and subjected to clean-up with solid phase extraction cartridges (SPE; RP-18; 6 mL, 500 mg). The stationary phase cartridge was activated with 10 mL methanol and conditioned with 20 mL of acidified water (0.05% formic acid). Subsequently, 1 mL of extract was applied to the cartridge and eluted with acidified water, 20% methanol (MeOH: acidified H_2O; v:v), 75% methanol (MeOH: acidified H_2O; v:v) and acidified methanol. Next, the fraction eluted with 75% methanol was dried in a vacuum solvent evaporator (SpeedVac®) at room

temperature. The fraction extracted with MC was re-solubilized in 1 mL of 50% methanol (MeOH:H_2O; v:v) and filtered through nylon filters (0.20 μm). The chromatographic separation and MC identification were performed as described in Section 2.2.

The MC concentration was quantified, in triplicate, using an HPLC connected to an API 2000™ triple Quadrupole Mass Spectrometer (AB/MDS Eciex, CA, USA) with a TurbolonSpray electrospray interface (ESI–MS) using a standard mixture (500 ng mL^{-1}) of MC-RR and MC-YR (Sigma-Aldrich, USA). The ESI source was used in positive multiple reaction-monitoring (MRM) mode. The HPLC/ESI–MS/MS analysis of MCs was conducted under the following conditions: declustering potential, 40 V; focusing potential, 400 V; collision energy, 40 V; cell entrance potential, 11 V, cell exit potential, 2 V; TurboIonSpray voltage, 4500 V; turbo temperature, 400 °C; nebulize gas (N_2), 55 psi; heated gas, 60 psi; curtain gas, 30 psi; and collision-activated dissociation, 8 psi. The MC quantification was achieved through external calibration using analytical curves of standard solutions containing MC-RR and MC-YR obtained from transition *m/z* 520 ($[M+2H]^{+2}$) and 534 ($[M+H+Na]^{+2}$), respectively, and *m/z* 135 transition from fragment ADDA(-(2S, 3S, 8S, 9S)-3-Amino-9-methoxy-2,6,8-trimethyl-10-phenyl-deca-4,6-dienoic acid). The precision (repeatability degree) was evaluated as intra-day (1.41 – 3.83% and 2.39 –4.79% for MC-RR and MC-YR, respectively). The accuracy (91.59 – 101.85% and 87.82 – 103.09% for MC-RR and MC-YR, respectively) was calculated by averaging the calculated concentrations and the average value of the nominal concentrations. In agreement with the FDA (2013) guidelines, the mean value for accuracy was within 15% of the nominal value. The limit of detection (LOD, 2 ng g^{-1} and 5 ng g^{-1} for MC-RR and MC-YR, respectively) was considered as three times the signal/noise ratio (S/N), and the limit of quantification (LOQ, 20 ng g^{-1} and 50 ng g^{-1} for MC-RR and MC-YR, respectively) was 10 times the S/N ratio. The selectivity of the method was characterized by assessing accurate quantification of MC-RR and MC-YR in the presence of endogenous compound, confirmed by the analysis of the blank. Recovery experiments were performed through fortification in triplicate fish samples (liver and muscle) with mixed MC solution (MC-RR and MC-YR).

2.5. Endogenous liver protein phosphatase activity

Liver samples were homogenized in ice cold buffer (40 mM Tris–HCl, 20 mM KCl, 30 mM $MgCl_2$, pH 8.6 with 2 mM PMSF) (1:4 w/v) using an Ultra Turrax homogenizer. Homogenates were centrifuged at 12,000*g*, 4 °C for 15 min and the supernatants were used as PP1 and PP2a enzyme sources. PP1 and PP2A activities (nmol min^{-1} mg $protein^{-1}$) were measured in a microplate reader using *p*-nitrophenyl phosphate (pNPP) as a substrate, according to Carmichael and An (1999) and Heresztyn and Nicholson (2001), respectively, adapted by Bieczynski et al. (2013). The absorbance was read at 405 nm, in triplicate, every 10 min for 60 min at 25 °C. The protein concentration in the homogenate was determined using Bradford reagent with bovine serum albumin as a standard (Kruger, 1994) at 595 nm.

2.6. Liver morphological analysis

The hepatosomatic index (HIS) was calculated as HSI = fresh liver mass/fresh body mass*100 according to Ratton et al. (2003).

LM analyses were used to evaluate liver histomorphology, collagen fibers and cell proliferation. For histomorphology, the liver samples fixed in 2.5% glutaraldehyde in 0.1 M phosphate buffer, pH 7.3 were dehydrated in ethanol crescent series, embedded in historesin (Leica, Germany) and the sections (3 μm in thickness) were stained with Toluidine blue and basic fuchsin. For identification of collagen fibers, the liver samples fixed in Bouin's solution were dehydrated in ethanol crescent series, embedded in paraffin and serial sections (6 μm in thickness) were stained with Masson's trichrome (EasyPath kit, Brazil). Cell proliferation was evaluated applying immunohistochemistry against proliferating cell nuclear antigen (PCNA); the liver samples fixed in Bouin's solution were processed as described above for embedding in paraffin and sectioned with 8 μm in thickness. Briefly, endogenous peroxidase activity was blocked with 1% hydrogen peroxidase and heated in 1% $ZnSO_4$, followed by cooling with distilled cold water for antigen retrieval. Subsequently, the sections were washed in Tris-buffered saline containing 0.1% Triton X-100 (TBS-T) and incu-

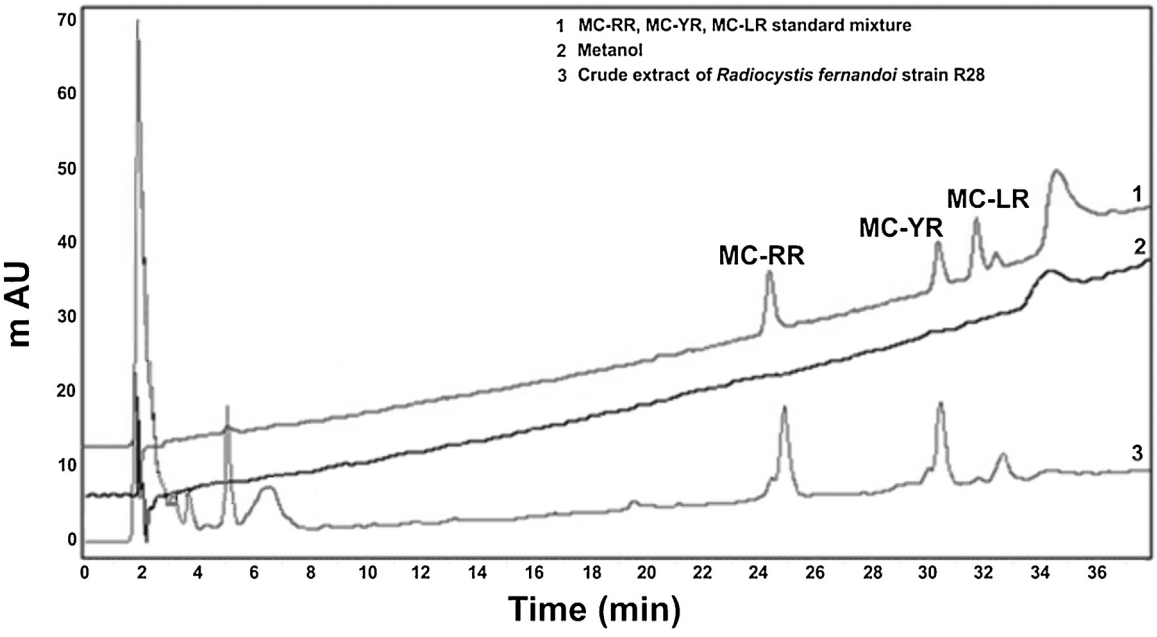

Fig. 1. HPLC chromatograms of microcystin in the crude extract of *Radiocystis fernandoi* strain R28, blank (methanol) and standard microcystin mixtures monitored at UV 240 nm.

bated with primary antibody PC10 (1:100 Immuny, Rheabiotech, Brazil), overnight in a wet chamber. After washing in TBS-T, a goat anti-mouse peroxidase conjugated secondary antibody (GAMPO, 1:2000) was added, and the sections were incubated for 1 h. The antibody complex was visualized by staining the sections with 0.5% DAB (3,3′-diaminobenzidin). For the negative controls, the primary or secondary antibodies were omitted, and the samples were incubated and stained as described above. PCNA-positive nuclei were expressed as a percentage of those in the control group. All morphological analyses were performed under an Olympus BX51 (Olympus, Denmark) light microscope equipped with a camera connected to a computer using Olympus DP2-B5W software and a randomized blind method with a range of 5 fields per section (n = 5) for each fish.

For TEM analyses, the liver samples fixed in 2.5% glutaraldehyde in 0.1 M phosphate buffer, pH 7.3, were post-fixed in 1% osmium tetroxide and block contrasted with 0.5% uranyl acetate in 10.5% sucrose. The samples were dehydrated in an acetone crescent series and embedded in Spurr's resin (EMS – Low Viscosity Embedding Media, U.S.). Ultrathin sections (60 nm in thickness) were contrasted with 3% uranyl acetate and 0.01% lead citrate. The images obtained from a transmission electron microscope (Philips CM-120, USA) at 80 kV using a range of 5 fields per 5 sections (n = 5) were analyzed for each fish.

2.7. Statistical analyses

The results are presented as the means ± S.E.M. Data normality was verified using the D'Agostino-Pearson test. Differences between acute exposure groups were analyzed with ANOVA, followed by Bonferroni's post-test. Differences between chronic exposure groups were analyzed using a *t*-test. All tests were performed using GraphPad Prism software (version 5.0) and data significance was designated at $p < 0.05$.

Table 1
Microcystin (MC) accumulation in the liver and muscle of *Hoplias malabaricus* from crude extract group (CE, *Radiocystis fernandoi* strain R28 crude extract injected) after acute (one single dose injection, 12 h and 96 h post-injection) and subchronic (one dose injection every 72 h, for 30 d) exposure.

Microcystin Accumulation				
CE Groups	MC-RR (ng mg tissue^{-1})		MC-YR (ng mg tissue^{-1})	
	Liver	Muscle	Liver	Muscle
Acute exposure				
12 h	–	–	135.7 ± 17. 2	–
96 h	–	–	47.4 ± 8.8	–
Subchronic exposure				
30 d	21.9 ± 0.07	–	44.4 ± 0.7	–

CE group (n = 3 pools); (–) indicate MC lower than detection/quantification limit.

3. Results

No fish died during acute and subchronic exposure experiments, and no changes in fish color or behavior were observed. During subchronic exposure, fish i.p. injected with crude extract showed a slight reduction in feeding.

3.1. MC-YR and MC-YR in R. fernandoi strain R28 crude extract and accumulation in fish liver and muscle

The similarity of chromatograms peaks in the HPLC suggested the presence of variants MC-RR and MC-YR and the absence of MC-LR in the crude extracts of *R. fernandoi* strain R28 (Fig. 1). The relative retention times of MC-RR and MC-YR were 24.3 and 30.5 min, respectively. The MC content in *R. fernandoi* crude extract was 2.40 mg of MC, comprising 1.46 mg of MC-RR and 0.94 mg of MC-YR per gram of freeze-dried cyanobacterial cells.

After 12 and 96 h crude extract injection (acute exposure) the MC-RR were identified in the liver, but this accumulation was not quantified because the amount was lower than the quantification

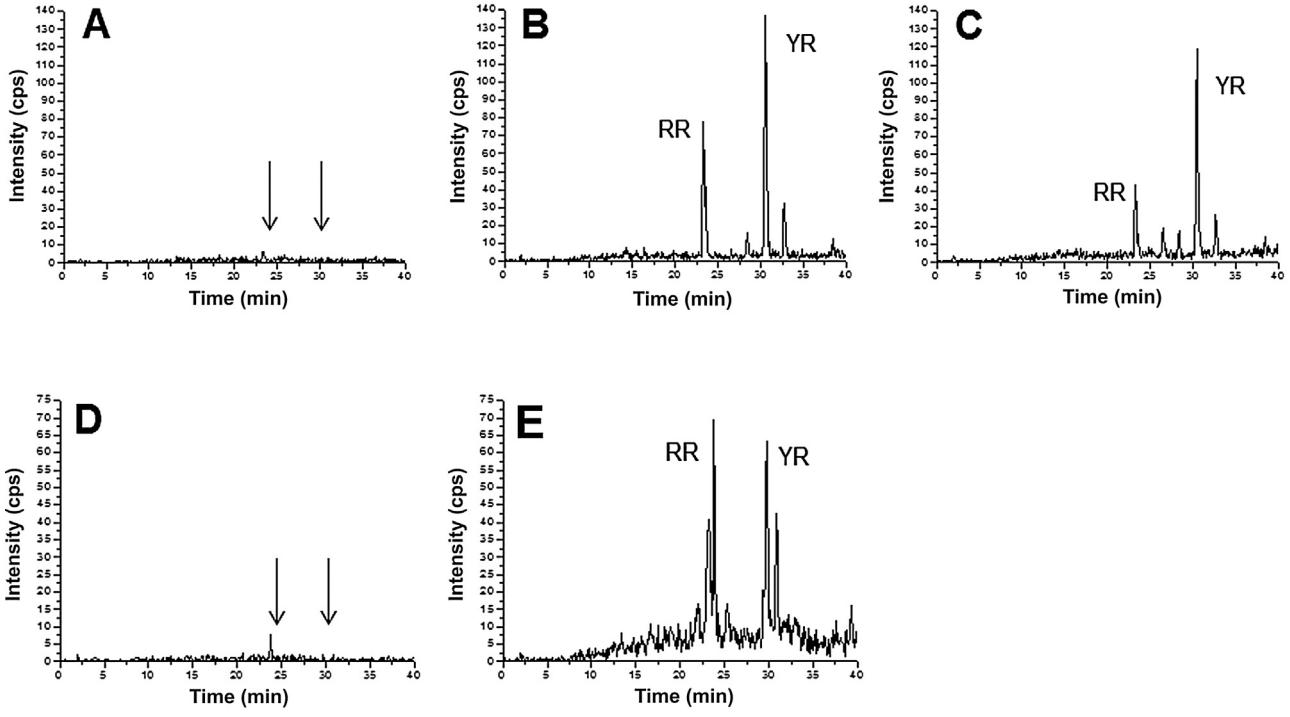

Fig. 2. MRM chromatograms of liver extract of *Hoplias malabaricus* from control group (C, saline injected) and crude extract group (CE, *Radiocystis fernandoi* strain R28 crude extract injected) after acute (one single dose injection; 12 h and 96 h post-injection) and subchronic (one dose injection every 72 h for 30 d) exposure. (A) Control 12 and 96 h; (B) CE 12 h; (C) CE 96 h; (D) Control 30 d and, (E) CE 30 d. The detection parameters are described in the Materials and Methods section.

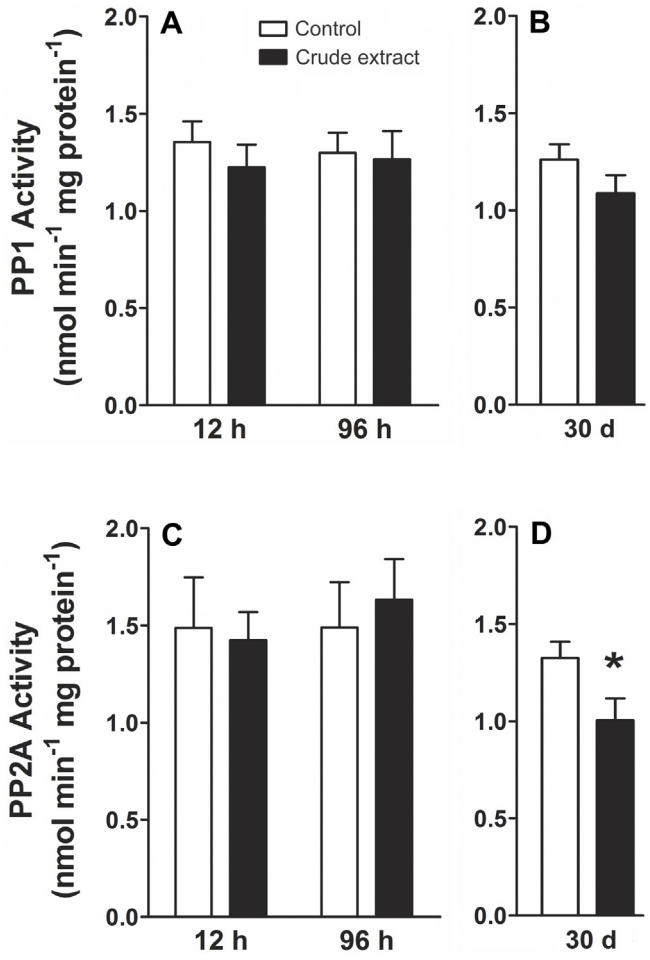

Fig. 3. Endogenous activity of protein phosphatase (PP1 and PP2A) in the liver of *Hoplias malabaricus* (n = 10) from control group (C, saline injected) and crude extract group (CE, *Radiocystis fernandoi* strain R28 crude extract injected) after acute (one single dose injection; 12 h and 96 h post-injection): A and C, respectively and, subchronic (one dose injection every 72 h for 30 d): B and D, respectively. The values are expressed as the mean ± SEM. *Indicates significant difference from respective control.

limits. Nevertheless, MC-YR accumulated in the liver at a concentration three times higher after i.p. crude extract injection for 12 h compared with 96 h (Table 1, Fig. 2). After subchronic exposure, both MC-RR and MC-YR accumulated in the liver; the MC-YR concentration was two times higher than the MC-RR concentration (Table 1). There was no accumulation of MCs in the white muscles, the edible part of fish (Table 1).

3.2. Endogenous PP1 and PP2A enzyme activity

The PP1 and PP2A activities unchanged after 12 and 96 h i.p. injection of the crude extract of *R. fernandoi* containing mostly MC-RR and MC-YR (acute exposure) (Fig. 3A, C). After subchronic exposure, PP1 activity remained unaffected; however, the activity of PP2A was significantly inhibited (Fig. 3B, D).

3.3. Liver morphological alterations

The fish body mass remained unchanged in either acute or subchronic exposed groups; whereas, the liver mass increased (155%) after 96 h exposure to *R. fernandoi* crude extract resulting in a HSI two times higher than that from control fish. However, after subchronic exposure, the liver mass decreased (29%) resulting in a HSI 0.6 lower than the controls (Table 2). Macroscopically, the liver from control fish presented an homogeneous aspect with a reddish-brown color (Fig. 4A), while the livers of fish exposed to *R. fernandoi* crude extract presented a yellowish color and hemorrhages at 12 and 96 h after i.p. injection (Fig. 4B and C) with a reddish-brown color and numerous dark blood spots after 30 days exposure (Fig. 4D).

The crude extract induced several changes in the structure of the liver at microscopic and ultrastructure levels (Fig. 5 and 6). The normal liver (control groups) showed homogenous distribution of hepatocytes and low connective tissue between these cells and the blood vessels (Fig. 5A, B). The hepatocytes were organized in a cord-like structure around sinusoid capillaries; they exhibited a polyhedral shape with well-defined cell limits and a central nucleus with a prominent nucleolus (Fig. 5A). Acute exposure caused alterations in the liver parenchyma that increased from 12 to 96 h. After 12 h crude extract i.p. injection, the hepatocytes presented a round shape and the loss of cord-like arrangement, peripheral nuclei, sinusoid enlargement and increased extracellular spaces (Fig. 5C). After 96 h, the sinusoids significantly increased (Fig. 5D), and some fibroblasts were detected in the liver parenchyma around the hepatocytes (Fig. 5E). Subchronic exposure (30 days) resulted in the complete disarrangement of the liver architecture (Fig. 5F), and extensive hepatic areas exhibited collagen fibers (Fig. 5G). Cell proliferation remained unchanged in the livers of fish i.p. injected with *R. fernandoi* crude extract after acute and subchronic exposure compared with fish i.p. injected with saline (controls) (Fig. 6).

At the ultrastructural level, the hepatocytes from control groups had nuclei with some condensed chromatin underneath the nuclear membrane and nucleolus. Abundant glycogen and several lipid drops of different in sizes were distributed throughout the cytoplasm, numerous mitochondria and abundant endoplasmic reticulum were localized around the nuclei and beneath the membrane perimeter (Fig. 7A and B), and a well-defined Golgi apparatus was around nuclei (Fig. 7C). The cell limits were clearly identified, and the bile canaliculus between hepatocytes was characterized by microvilli in the lumen of the canaliculus and junction complexes (Fig. 7D). After acute and chronic exposure to crude *R. fernandoi* extract, the hepatocytes structure changed. Twelve hours after i.p. crude extract injection, rounded hepatocytes presented extended chromatin throughout the nucleus, most of which showed reduced sizes or the absence of a nucleolus; cytoplasmic disorganization

Table 2
Body and liver mass and hepatosomatic index (HSI) of *Hoplias malabaricus* (n = 10) from control (C, saline injected) and crude extract group (CE, *Radiocystis fernandoi* strain R28 crude extract injected) after acute (a single dose injection; 12 h and 96 h post-injection) and subchronic (one dose injection every 72 h for 30 d) exposure. Values are mean ± SEM.

	Acute exposure				Subchronic exposure	
	C12 h	CE12 h	C96 h	CE96 h	C30 d	CE30 d
Initial body mass (g)	261.1 ± 35.05	247.0 ± 33.29	264.8 ± 39.53	237.2 ± 23.15	271.4 ± 13.52	301.9 ± 20.62
Final body mass (g)	243.5 ± 31.30	242.2 ± 31.95	245.0 ± 34.95	222.3 ± 21.97	279.1 ± 18.32	300.2 ± 16.24
Hepatic mass (g)	4.8 ± 1.18	6.2 ± 1.16	4.7 ± 1.06	7.3 ± 1.01[a]	4.2 ± 0.32	3.0 ± 0.45[a]
HSI (%)	1.8 ± 0.43	2.7 ± 0.58	1.9 ± 0.40	3.3 ± 0.40[a]	1.5 ± 0.07	0.9 ± 0.10[a]

[a] Indicates significant difference from the respective control group ($p < 0.05$).

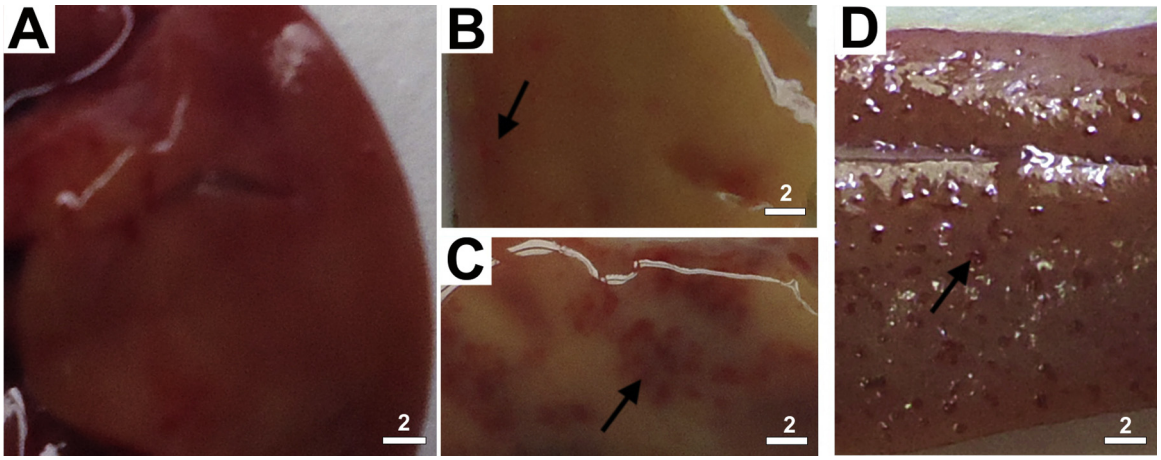

Fig. 4. Macroscopic view of *Hoplias malabaricus* liver. A. Control group (saline injected) and B-D, crude extract group (*Radiocystis fernandoi* strain R28 crude extract injected) after acute (one single dose injection; 12 h and 96 h post-injection, B and C) and subchronic (one dose injection every 72 h for 30 d, D) exposure. Note the yellowish color in B, hemorrhages areas (arrow) in B and C and dark blood spots (arrow) in D. Scale bars are in mm. (For interpretation of the references to colour in this figure legend, the reader is referred to the web version of this article.)

was characterized by glycogen and lipid droplets depletion, electron lucent vacuoles and shrunken cytoplasmic organelles around the nucleus (Fig. 8A-C). Mitochondrial swelling and extensive endoplasmic reticulum disorganization (Fig. 8C) were common features in the hepatocytes after 12 h (Fig. 8C), and cells exhibiting advanced necrotic features were observed after 12 and 96 h exposures (Fig. 8D, E). Disrupted cellular membranes were common features of the hepatocytes after 96 h (Fig. 8E), and many hepatocytes contained electron dense bodies and concentric layers of membranes resembling myelinated bodies (Fig. 8F). Some hepatocytes maintained organized mitochondria around the nucleus and presented blebbing of the cellular membrane (Fig. 8G). In the extracellular space, numerous vacuolated materials and some fibroblasts were observed (Fig. 8H).

After subchronic exposure, despite hepatic cells showed a round shape and organelle disorganization, it was difficult to identify the cell outline. Some of the hepatocytes had endoplasmic reticulum and normal mitochondria around the nucleus (Fig. 9A and B). Most of the endoplasmic reticulum exhibited whirling features (Fig. 9B). Connective cells and large amounts of collagen fibers characterized the liver parenchyma (Fig. 9C and D).

4. Discussion

The present study is the first to examine in fish the toxicity of *R. fernandoi* strain R28, a common cyanobacterium and MC-RR and MC-YR producer in blooms in Neotropical regions. MC-RR is the one of the dominant variants in the lakes of China (Xie et al., 2015) and, despite the abundance of the RR form, there are few studies on the toxicity of this variant; MC-YR is less produced by cyanobacteria than MC-LR and MC-RR (WHO, 1998).

The differences in MC-RR and MC-YR accumulation in the liver of *H. malabaricus* likely reflect the hydrophilic/hydrophobic characteristics or metabolism/excretion efficiency following acute and subchronic fish contamination. Consequently, the crude extracted toxicity showed time-dependent changes in the liver and hepatocytes at 12 and 96 h after a single dose injection (acute exposure) and a dose injection every 72 h for 30 days (subchronic exposure). The replacement of the amino acid leucine in position 2 in the MC-LR by tyrosine in MC-YR or arginine in MC-RR change the hydrophobic characteristics of MC molecule and, consequently, the absorption, metabolism and toxicity of these variants (Gehringer et al., 2005). A comparison between the toxicity of MC-LR and that of MC-RR and MC-YR in mice revealed that the $LD_{50;}$ 24 h increased from 43 to 111 and 235 $\mu g\,kg^{-1}$ body mass for MC-LR, MC-YR and MC-RR, respectively, showing that less hydrophobic MC variants have lower toxicity (Gupta et al., 2003).

The hydrophilic characteristic of MC-RR favors its metabolism and fast transportation to the kidneys, where this variant is excreted (Wu et al., 2013), which might explain the identification of MC-RR in the liver of *H. malabaricus* 12 and 96 h after i.p. injection at a lower level than the quantification limit. However, after subchronic exposure, the continuous MC contamination of fish for 30 days resulted in MC-YR and MC-RR accumulation in the liver suggesting that the depuration is not fast enough to avoid MC accumulation in liver under continuous contamination. In general, independent of the absorption route, the MC accumulation was higher in the liver than in other organs (Deblois et al., 2011; Xie et al., 2004). The accumulation of MC in different tissues depends on tissue metabolism/excretion capability and/or the presence/absence of expression of organic anion-transporting polypeptide (Oatp) types which transport MC into the cell (Dietrich and Hoeger, 2005; Popovic et al., 2010). The lack of MC accumulation in the muscles of *H. malabaricus*, even after subchronic exposure, may be related to Oatps in the muscle cells.

MC toxicity has been associated with the interaction of MC molecules with PP1 and PP2A, which promotes the phosphorylation of the cellular proteins responsible for many signal transduction responses (Buratti et al., 2013). PP1 and PP2A are inhibited because of interactions with the hydrophobic region of Adda, the glutamyl carboxylate and the methyldehydro-Ala of MC (Hastie et al., 2005). The variable amino acids from the MC molecule are not critical for the protein phosphatase inhibition (Heussner et al., 2014; MacKintosh et al., 1995), although, crucial to toxicity, and the toxicity of MC decreases from MC-LR to MC-YR and MC-RR (Buratti et al., 2013; Covaci et al., 2012). The absence of PP1 and PP2A inhibition 12 and 96 h after *R. fernandoi* crude extract injection in *H. malabaricus* probably reflected the reversible binding of MC with these phosphatases. In general, the maximum PP inhibition occurs between 3 and 6 h after fish MC contamination (Malbrouck et al., 2004; Tencalla and Dietrich 1997). In trout, *Oncorhynchus mykiss*, the inhibition of PP activity (60%) was observed up to 3 h post-gavage, followed by gradual recovery until 72 h (Tencalla and Dietrich, 1997), and in goldfish, *Carassius auratus,* the inhibition of PP activity primarily occurred at 6 h post-gavage and was completely recovered after 96 h Malbrouck et al. (2004). Furthermore, MC underwent rapid covalent binding with cysteine (Cys) and glutathione (GSH) favoring metabolism and excretion of tox-

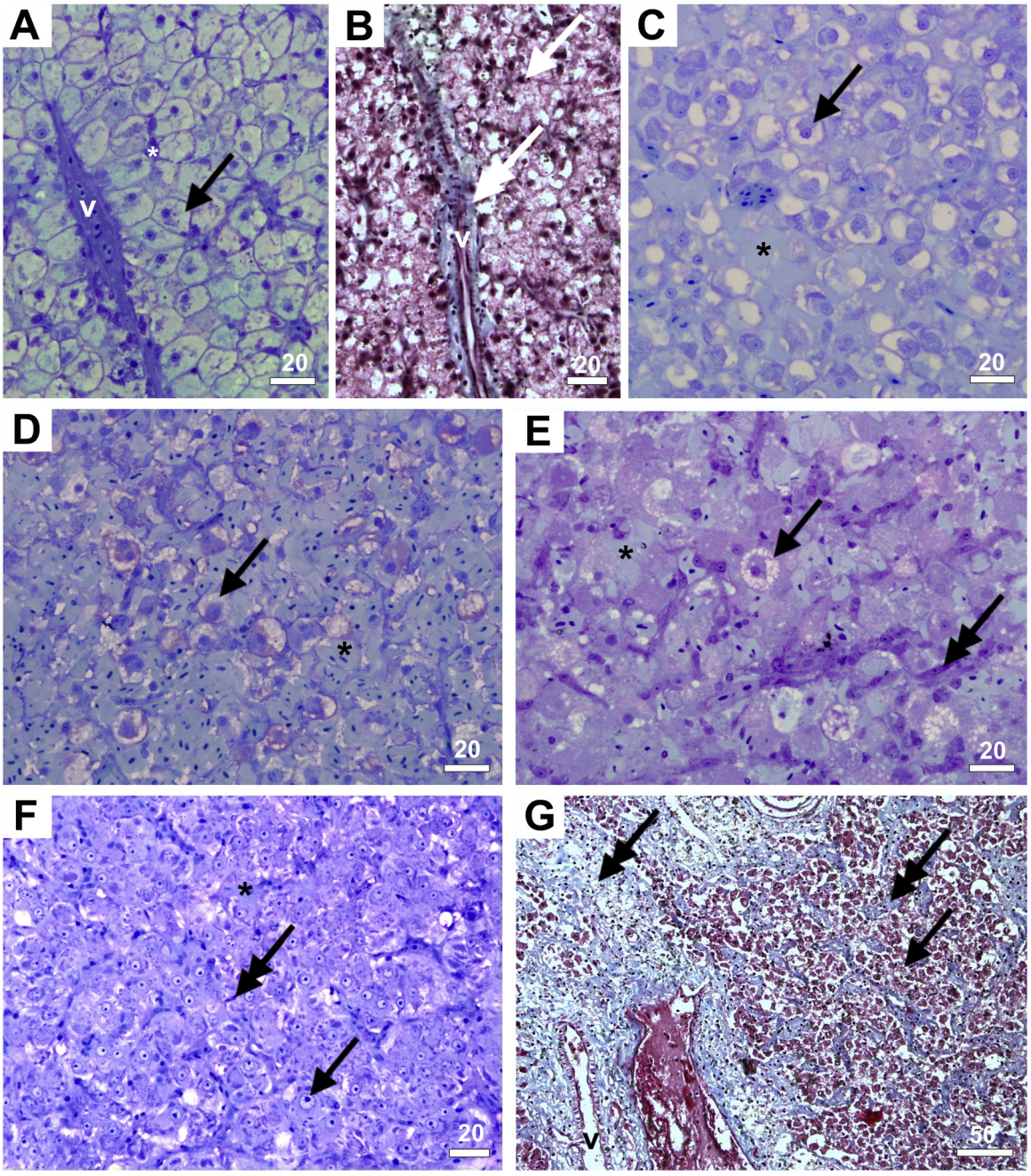

Fig. 5. Microscopic view of *Hoplias malabaricus* liver. A and B, control group (saline injected), normal liver; note hepatocytes shape (arrow) and cord-like organization, sinusoid (*) in A and connective tissue (double arrow) close to blood vessels in B. C-G, crude extract exposure (*Radiocystis fernandoi* strain R28 crude extract injected): acute exposure (a single dose injection) 12 h (C) and 96 h (D and E) post-injection and subchronic exposure (one dose injection every 72 h) 30 d post-injection (F and G). Note rounded hepatocytes (arrow) and sinusoids intercellular space (*) in C; highly increasing of enlarged sinusoids (*) in D and fibroblasts (double arrow) among hepatocytes (arrow) in E; hepatocytes showing hypertrophied nucleus (arrow) and fibroblast (double arrow) among them in F and large amount of connective tissue in G. v vessels. A, C-E, toluidine blue and basic fucsine stain; B and G, Masson's trichrome stain. Scale bars are in μm. (For interpretation of the references to colour in this figure legend, the reader is referred to the web version of this article.)

ins and metabolites which may reduce the MC action on the PP. Nevertheless, PP inhibition in both fish and mammals is time/dose-dependent (Cohen et al., 1988; Runnegar et al., 1993 Runnegar et al., 1993). In the present study, the inhibition of PP2A activity in the liver of *H. malabaricus* after subchronic exposure, suggests that the MC-RR and MC-YR accumulation in this organ overcomes its capability to metabolize and excreted MC resulting in PP inhibition under continuous contamination.

The overall changes in the liver of *H. malabaricus* after *R. fernandoi* crude extract i.p. injection suggesting toxicity was macroscopically observed based on varying color, mass and tissue characteristics as already reported by Molina et al. (2005) in *Oreochromis niloticus* exposed to the MC during cyanobacterial blooms. The increasing liver mass and HSI after 96 h likely reflected the intense blood flow into the liver, which was confirmed after microscopic analyses. Notably, the blood flow was highly dispersed after 12 h and more localized in some liver areas after 96 h exposure, despite the sharp decrease of hepatic glycogen after acute exposure, as observed in the hepatocyte ultrastructure. HSI is typically associated with the nutritional state and energy reserves as the

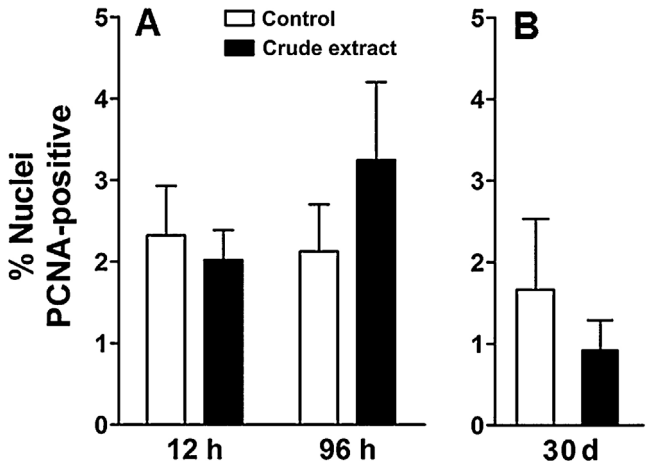

Fig. 6. PCNA-positive cells in the liver of *Hoplias malabaricus* (n = 10) from control groups (saline injected) and crude extract groups (*Radiocystis fernandoi* strain R28 crude extract injected): acute exposure (a single dose injection) 12 h and 96 h post-injection (A) and subchronic exposure (one dose injection every 72 h) 30 d post-injection (B). The values are expressed as the means ± SEM. *Indicates significant difference from respective control.

storage of large amounts of glycogen and lipids inside hepatocytes. However, stressful conditions induce variations in these reserves and consequently in HSI (Querol et al., 2002). Increasing HSI after acute exposure (24 h) to *Microcystis* extract containing MC and lipopolysaccharides from the cyanobacteria cell surface was reported in *Oncorhynchus mykiss* (Best et al., 2003), and no changes in the HSI were observed in *Coregonus lavaretus* at 72 h after oral (gavage) exposure to whole cyanobacterial cells (Ernst et al., 2006). In *H. malabaricus*, the maintenance of hyperemia and the replacement of hepatocytes by collagen fibers after continuous exposure to crude cyanobacterial extract resulted in decreased liver mass and HSI. Similarly, a decrease in HSI was reported in *Oreochromis niloticus* after subchronic exposure (10 days) to crude cyanobacterial extract (Ibrahem et al., 2012), and these effects likely reflected liver impairment. These results suggest that the modality of exposure is an important factor facilitating the uptake of toxins and other cyanobacterial components affecting the liver.

Changes in the liver parenchyma and the histological and ultrastructural features of hepatocytes were time- and form-exposure dependent. Changes in shape of hepatocytes from polyhedral to rounded cells and the disjunction of cellular adhesion, which increased the intercellular space, might reflect the disorganization of polymer proteins, components of the cellular cytoskeleton (Fischer et al., 2000). This effect causes blood increase in the sinusoids leading to hyperemia and bleeding in liver. Such effects are characteristic of the toxicity of MC-RR and MC-YR in the crude extract of *R. fernandoi* and have been reported in numerous fish species exposed to cyanobacterial extracts or natural blooms. This toxicity leads to hypovolemic shock and death, depending on the dose and exposure time (Atencio et al., 2009; Ernst et al., 2006; Li et al., 2007; Marie et al., 2012).

The sequence of events in the liver at 12 to 96 h post i.p. extract injection revealed a progressive effect of the MCs present in crude extract that were consistent with the findings of Fischer et al. (2000) and Li et al. (2005, 2001). Increased energy mobilization was evidenced by a decrease in glycogen and lipid droplets and cytoplasmic vacuolization after 12 h, which were followed by the

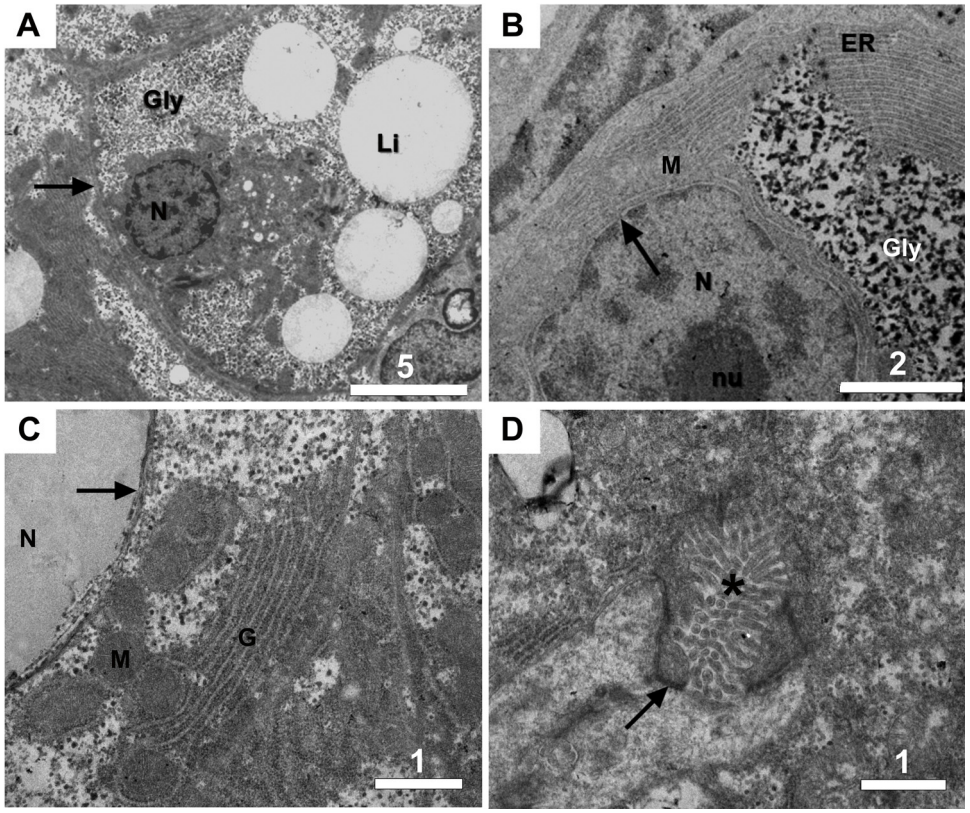

Fig. 7. TEM micrographs of the normal hepatocyte ultrastructure of *Hoplias malabaricus* (Control, saline injection). A. Hepatocyte showing nucleus, glycogen distributed throughout cytoplasm and lipid droplets and a well-defined cell membrane (arrow); B. Extensive endoplasmic reticulum and glycogen and nuclear pore (arrow) in the nuclear membrane; C. Mitochondria around the nucleus and Golgi apparatus, nuclear pore (arrow) in the nuclear membrane; D. High magnification of the bile canaliculus filled with hepatocyte microvilli (*) and junctional complexes (arrow). ER – endoplasmic reticulum, G – Golgi apparatus, Gly – glycogen, Li – lipid, M – mitochondria, N – nucleus, nu – nucleolus. Scale bars are in μm.

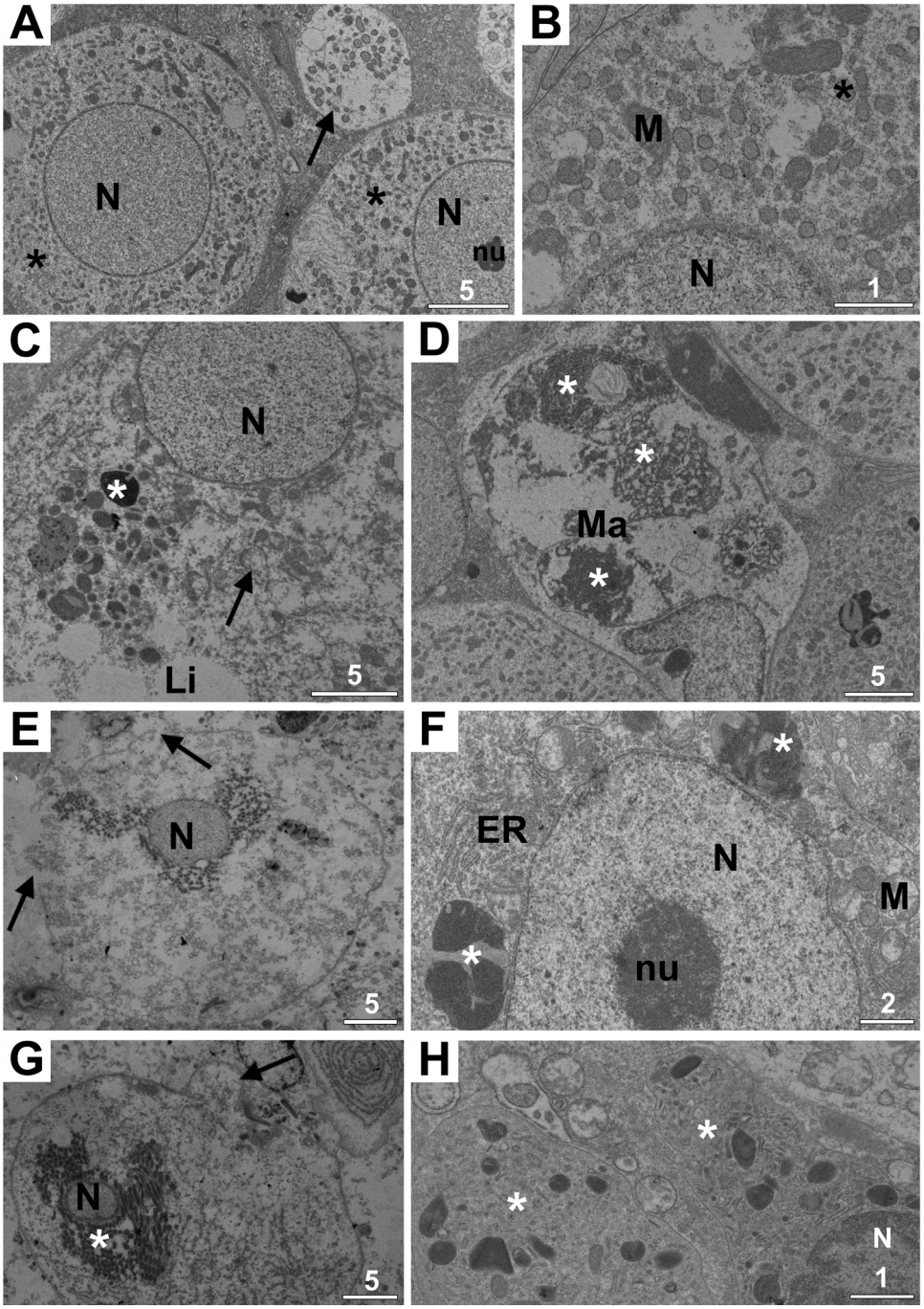

Fig. 8. TEM micrographs of the liver of *Hoplias malabaricus* injected with crude extract of *Radiocystis fernandoi* strain R28: acute exposure (a single dose injection) 12 h (A-D) and 96 h (E-H) post-injection. A. Round hepatocytes showing the nucleus and nucleolus and electron lucent cytoplasm (*), necrotic bodies (arrow) in the extracellular space; B. High magnification of a hepatocyte showing numerous dispersed vesicles (*); C. Hepatocyte with altered organelles (arrow) and condensed bodies (*) in the cytoplasm; D. Macrophage (Ma) with cellular bodies (*); E. Disruption of the plasma membrane (arrow) in necrotic hepatocytes; F. Endoplasm reticulum disorganization, swelled mitochondria (M) and electron dense bodies (*) around nucleus; G. Hepatocyte with disorganized cellular organelles (*) around the nucleus and blebbing of the cell membrane (arrow); H. Fibroblasts (*) in the intercellular space. ER – endoplasmic reticulum, N – nucleus, nu – nucleolus; M – mitochondria. Scale bars are in μm.

disorganization of endoplasmic reticulum, mitochondrial swelling and membrane rupture after 96 h exhibiting signs of necrosis. These severe injuries imply in impairments of energy production and alterations of cellular functions (Maioli et al., 2011) eventually leading to fish death due to extensive hepatic necrosis.

After subchronic exposure, the swollen mitochondria and degranulation, dispersion of the stacks and whirling endoplasmic reticulum in the hepatocytes of *H. malabaricus* suggested high damage in the liver, consistent with the reports of the hepatocytes of *Cyprinus carpio* exposed to 50 μg MC-LReq kg^{-1} for 28 days (Li et al., 2004). Furthermore, the overall reduction of enlarged sinusoids in the liver of *H. malabaricus* and the extensive increase of connective tissue among hepatocytes characterizing fibrosis was also other characteristic of liver damage after subchronic exposure to the crude extract of *R. fernandoi*, which, to our knowledge, has not yet been described in fish. The presence of liver fibrosis after subchronic MC exposure has only been reported in mammals (Falconer and Buckley, 1989; Gupta et al., 2003). Liver fibrosis has many

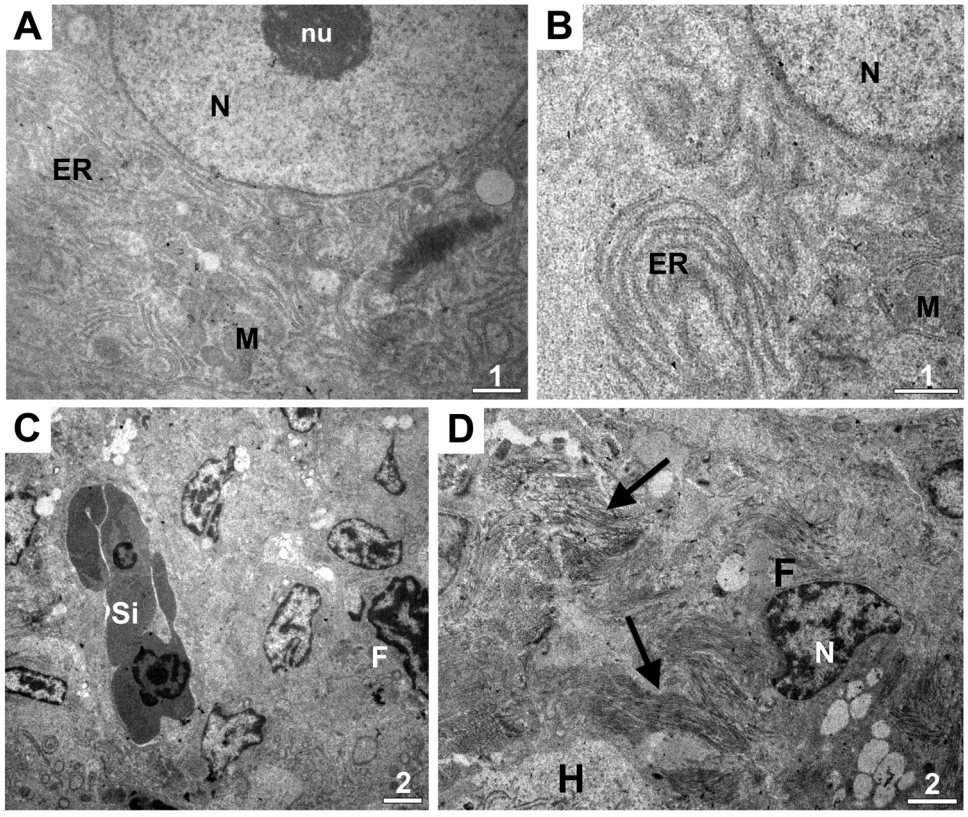

Fig. 9. TEM micrographs of the liver of *Hoplias malabaricus* injected with crude extract of *Radiocystis fernandoi* strain R28: subchronic exposure (one dose injection every 72 h for 30 d). A. Hepatocyte showing endoplasmic reticulum disorganization and mitochondria; B. High magnification of whirling endoplasmic reticulum and mitochondria; C. Liver parenchyma showing sinusoid (*) and fibroblasts; D. Collagen fibers (arrows) among hepatocytes and fibroblasts. ER – endoplasmic reticulum, F – fibroblast, H – hepatocytes, M-mitochondria; N – nucleus, Scale bars are in μm.

causes (Rose, 2002) and might reflect the collapse of the hepatic parenchyma and its substitution by collagen-rich tissue.

Although poorly documented, it is generally assumed that MC-LR is a potent tumor promoter (Menezes et al., 2013); however, no evidence of tumor induction was provided by MC-RR and MC-YR present in the crude extract of *R. fernandoi in this study*. This effect might involve many factors, such as dose, exposure time, input and MC metabolic capacity of different species

5. Conclusions

Radiocystis fernandoi strain R28 can be characterized as a toxic clade of microorganisms that primarily produce MC-RR and MC-YR. Although these variants are less toxic than MC-LR, this study supports the hypothesis that the exposure of fish to a mixture of MCs in natural blooms might produce similar effects as those produced by MC-LR, leading to serious structural changes and physiological impairments of the liver, depending on the concentration and exposure time. Furthermore, the decreased detoxification capacity of the liver and increased MC accumulation might be potential risks for human health, in the long-term, the accumulation may occurs in other tissues, such as muscles.

Acknowledgements

This study was supported by the Energetic Company of Minas Gerais (CEMIG, Proc. GT 346) and São Paulo State Funding Agency (FAPESP, Proc. 2012/00728-1), Brazil. The authors would like to thank the Center of Applied Ecology of Neuquen, Neuquen, Argentina, for providing research facilities. M.G. Paulino acknowledges CEMIG (Proc GT 346) and FAPESP (Proc. 2012/00728-1), N.E.S. Souza, P.G. Pedrão, D. Tavares and A.P. Terezan acknowledge CEMIG (Proc GT 346) and M.M. Sakuragui acknowledges the Coordenação de Aperfeiçoamento do Pessoal Docente CAPES/PNPD (Proc. 2276/2011), Brazil, for scholarships.

References

Andrinolo, D., Sedan, D., Telese, L., Aura, C., Maser, S., Giannuzzi, L., Marra, C.A., Alanizc, M.J.T., 2008. Hepatic recovery after damage produced by sub-chronic intoxication with the cyanotoxin microcystin LR. Toxicon 51, 457–467.

Aranda-Rodriguez, R., Tillmanns, A., Benoit, F.M., Pick, F.R., Harvie, J., Solenaia, L., 2005. Pressurized liquid extraction of toxins from cyanobacterial cells. Environ. Toxicol. 20, 390–396.

Atencio, L., Moreno, I., Jos, A., Prito, A., Moyano, R., Blanco, A., Cameán, A.M., 2009. Effects of dietary selenium on the oxidative stress and pathological changes in tilapia (*Oreochromis niloticus*) exposed to a microcystin-producing cyanobacterial water bloom. Toxicon 53, 269–282.

Best, J.H., Eddy, F.B., Codd, G.A., 2003. Effects of Microcystis cells, cell extracts and lipopolysaccharide on drinking and liver function in rainbow trout *Oncorhynchus mykiss* Walbaum. Aquat. Toxicol. 64, 419–426.

Bieczynski, F., Bianchi, V.A., Luquet, C.M., 2013. Accumulation and biochemical effects of microcystin-LR on the Patagonian pejerrey (*Odontesthes hatcheri*) fed with the toxic cyanobacteria *Microcystis aeruginosa*. Fish. Physiol. Biochem. 39, 1309–1321.

Bieczynski, F., De Anna, J.S., Pirez, M., Brena, B.M., Villanueva, S.S.M., Luquet, C.M., 2014. Cellular transport of microcystin-LR in rainbow trout (*Oncorhynchus mykiss*) across the intestinal wall: possible involvement of multidrug resistance-associated proteins. Aquat. Toxicol. 154, 97–106.

Borges, P.A.F., Train, S., Rodrigues, L.C., 2008. Estrutura do fitoplâncton, em curto período de tempo, em um braço do reservatório de Rosana (ribeirão do Corvo, Paraná, Brasil). Acta Sci. Biol. Sci. 30, 57–65.

Buratti, F.M., Scardala, S., Funari, E., Testai, E., 2013. The conjugation of microcystin-RR by human recombinant GST's and hepatic cytosol. Toxicol. Lett. 219, 231–238.

Carmichael, W.W., An, J., 1999. Using an enzyme linked immunosorbent assay (ELISA) and a protein phosphatase inhibition assay (PPIA) for the detection of microcystins and nodularins. Nat. Toxins 7, 377–385.

Carmichael, W.W., Azevedo, S.M.F.O., An, J.S., Molica, R.J.R., Jochimsen, E.M., Lau, S., Rinehart, K.L., Shaw, G.R., Eaglesham, G.K., 2001. Human fatalities from

cyanobacteria: chemical and biological evidence for cyanotoxins. Environ. Health Perspect. 109, 663–668.
Carmichael, W.W., 1997. The cyanotoxins. Adv. Bot. Res. 27, 211–256.
Cohen, P.S., Alemany, S., Hemmings, B.A., Resink, T.J., Stralfors, P., Tung, H.Y.L., 1988. Protein phosphatase 1 and protein phosphatase 2A from rabbit skeleletal muscle. Methods Enzymol. 159, 390–408.
Covaci, O.I., Sassolasw, A., Alonso, G.A., Muñoz, R., Radu, G.L., Bucur, B., Marty, J.-L., 2012. Highly sensitive detection and discrimination of LR and YR microcystins based on protein phosphatases and na artificial neural network. Anal. Bioanal. Chem. 404, 711–720.
Deblois, C.P., Giani, A., Bird, D.F., 2011. Experimental model of microcystin accumulation in the liver of *Oreochromis niloticus* exposed subchronically to a toxic bloom of *Microcystis sp.* Aquat. Toxicol. 103, 63–70.
Dietrich, D.R., Hoeger, S.J., 2005. Guidance values for microcystin in water and cyanobacterial supplement products (blue-green algae supplements): a reasonable or misguided approach? Toxicol. Appl. Pharmacol. 203, 273–289.
Ernst, B., Hoeger, S.J., O'Brien, E., Dietrich, D.R., 2006. Oral toxicity of the microcystin-containing cyanobacterium *Planktothrix rubescens* in European whitefish (*Coregonus lavaretus*). Aquat. Toxicol. 79, 31–40.
FDA, 2013. Guidance for Industry, Bioanalytical Method Validation. U.S. Food & Drugs Administration, http://www.fda.gov/downloads/drugs/guidancecomplianceregulatoryinformation/guidances/ucm368107.pdf (Accessed 11 November 2016).
Falconer, I.R., Buckley, T.H., 1989. Tumor promotion by *Microcystis sp.* a bluegreen alga occurring in water supplies. Med. J. Aust. 150, 351–351.
Falconer, I.R., Yeung, D.S.K., 1992. Cytoskeletal changes in hepatocytes induced by microcystis toxins and their relation to hyperphosphorylation of cell proteins. Chem. Biol. Interact. 81, 181–196.
Fischer, W.J., Hitzfeld, B.C., Tencalla, F., Eriksson, J.E., Mikhailov, A., Dietrich, D.R., 2000. Microcystin-LR toxicodynamics, induced pathology, and immunohistochemical localization in livers of blue-green algae exposed rainbow trout (*Oncorhynchus mykiss*). Toxicol. Sci. 54, 365–373.
Fonseca, I.A., Maniglia, T.C., Rodrigues, L., Prioli, A.J., Prioli, S.M.A.P., 2011. Identificação do gene mcyA em florações naturais de *Radiocystis fernandoi*, em um tributário do reservatório de Rosana, Brasil. Acta Sci. Bioli Sci. 33, 319–324.
Gehringer, M.M., Milne, P., Lucietto, F., Downing, T.G., 2005. Comparison of the structure of key variants of microcystin to vasopressin. Environ. Toxicol. Pharmacol. 19, 297–303.
Gupta, N., Pant, S.C., Vijayaraghavan, R., Rao, P.V., 2003. Comparative toxicity evaluation cyanobacterial cyclic peptide toxin microcystins variants (LR, RR, YR) in mice. Toxicology 188, 285–296.
Hao, L., Xie, P., Fu, J., Li, G., Xiong, Q., Li, H., 2008. The effect of cyanobacterial crude extract on the transcription of GST mu, GST kappa and GST rho in different organs of goldfish (*Carassus auratius*). Aquat. Toxicol. 90, 1–7.
Hastie, C.J., Borthwick, E.B., Morrison, L.F., Codd, G.A., Cohen, P.T.W., 2005. Inhibition of several protein phosphatases by a noncovalently interacting microcystin and a novel cyanobacterial peptide, nostocyclin. Biochim. Biophys. Acta 1726, 187–193.
Heresztyn, T., Nicholson, B.C., 2001. Determination of cyanobacterial hepatotoxins directly in water using a protein phosphatase inhibition assay. Water Res. 35, 3049–3056.
Heussner, A., Altaner, S., Kamp, L., Rubio, F., Dietrich, D.R., 2014. Pitfalls in microcystin extraction and recovery from human blood sérum. Chem. Biol. Interact. 223, 87–94.
Ibrahem, M.D., Khairy, H.M., Ibrahim, M.A., 2012. Laboratory exposure of *Oreochromis niloticus* to crude microcystins (containing microcystin-LR) extracted from Egyptian locally isolated strain (*Microcystis aeruginosa* Kutzing): biological and biochemical studies. Fish. Physiol. Biochem. 38, 899–908.
Kruger, N.J., 1994. The Bradford method for protein quantification. Methods Mol. Biol. 32, 9–15.
Li, X.Y., Liu, Y.D., Song, L.R., 2001. Cytological alterations in isolated hepatocytes from common carp (*Cyprinus carpio* L.) exposed to microcystin-LR. Environ. Toxicol. 16, 517–522.
Li, X.Y., Chung, I.K., Kim, J.I., Lee, J.A., 2004. Subchronic oral toxicity of microcystin in common carp (*Cyprinus carpio* L.) exposed to *Microcystis* under laboratory conditions. Toxicon 44, 821–827.
Li, L., Xie, P., Chen, J., 2005. In vivo studies on toxin accumulation in liver and ultrastructural changes of hepatocytes of the phytoplanktivorous bighead carp i.p.-injected with extracted microcystins. Toxicon 46, 533–545.
Li, M., Satinover, D.L., Brautigan, D.L., 2007. Phosphorylation and functions of inhibitor-2 family of proteins. Biochemistry 46, 2380–2389.
MacKintosh, R.W., Dalby, K.N., Campbell, D.G., Cohen, P.T.W., Cohen, P., MacKintosh, C., 1995. The cyanobacterial toxin microcystin binds covalently to cysteine-273 on protein phosphatase 1. FEBS Lett. 371, 236–240.
Maioli, M.A., Alves, L.C., Perandin, D., Garcia, A.F., Pereira, F.T., Mingatto, F.E., 2011. Cytotoxicity of monocrotaline in isolated rat hepatocytes: effects of dithiothreitol and fructose. Toxicon 57, 1057–1064.
Malbrouck, C., Trausch, G., Devos, P., Kestemont, P., 2004. Effect of microcystin-LR on protein phosphatase activity in fed and fasted juvenile goldfish *Carassius auratus* L. Toxicon 43, 295–301.
Marie, B., Hueta, H., Marie, A., Djediat, C., Puiseux-Dao, S., Catherinea, A., Trinchet, I., Edery, M., 2012. Effects of a toxic cyanobacterial bloom (*Planktothrix agardhii*) on fish: insights from histopathological and quantitative proteomic assessments following the oral exposure of medaka fish (*Oryzias latipes*). Aquat.Toxicol. 114–115, 39–48.
Mekebri, A., Blondina, G.J., Crane, D.B., 2009. Method validation of microcystins in water and tissue by enhanced liquid chromatography tandem mass spectrometry. J. Chromatogr. A 1216, 3147–3155.
Menezes, C., Valério, E., Dias, E., 2013. The Kidney Vero-E6 Cell Line: A Suitable Model to Study the Toxicity of Microcystins. In: Gowder, S. (Ed.), New Insights into Toxicity and Drug Testing. InTech, Viena, pp. 29–48, http://dx.doi.org/10.5772/54463.
Molina, R., Moreno, I., Pichardo, S., Jos, A., Moyano, R., Monterde, J.G., Cameán, A., 2005. Acid and alcaline phosphatase activities and pathological changes induced in tilapia fish (*Oreochromis sp.*) exposed subchornically to microcystins from toxic cyanobacterial blooms under laboratory conditions. Toxicon 46, 725–735.
Nakatani, K., Agostinho, A.A., Baumgartner, G., Bialetzki, A., Sanches, P.V., Makrakis, M.C., Pavanelli, C.S., 2001. Ordem characiformes. In: Ovos e Larvas de Peixes de Água Doce: Desenvolvimento e Manual de Identificação. UEM, Maringá, pp. 73–220.
Palíková, M., Navrátil, S., Marsálek, B., Bláha, L., 2003. Toxicity of crude extract of cyanobacteria for embryos and larvae of carp (*Cyprinus carpio* L.). Acta Vet. Brno 72, 437–443.
Pereira, D.A., Giani, A., 2014. Cell density-dependent oligopeptide production in cyanobacterial strains. FEMS Microbiol. Ecol. 88, 175–183.
Pereira, D.A., Pimenta, A.D.C., Giani, A., 2012. Profiles of toxic and non-toxic oligopeptides of Radiocistis fernandoii (Cyanobacteria) exposed to three different light intensities. Microbiol. Res. 167, 413–421.
Pereira, D.A., Pimentel, J.S.M., Bird, D.F., Giani, A., 2015. Changes in oligopeptide production by toxic cyanobacterial strains under iron deficiency. Aquat. Microb. Ecol. 74, 205–214.
Popovic, M., Zaja, R., Smital, T., 2010. Organic anion transporting polypeptides (OATP) in zebrafish (*Danio rerio*): Phylogenetic analysis and tissue distribution. Comp. Biochem. Physiol. A 155, 327–335.
Querol, M.V.M., Querol, E., Gomes, N.N.A., 2002. Fator de condição gonadal, índice hepatossomático e recrutamento como indicadores do período de reprodução de *Loricariichthys platymetopon* (Osteichthyes, Loricariidae), bacia do rio Uruguai médio, Sul do Brasil. Iheringia. Série Zoologia 92, 79–84.
Ratton, F.T., Bazzoli, N., Santos, B.G., 2003. Reproductive biology of *Apareiodon affinis* (Pisces: Parodontidae) in the Furnas reservoirs, Minas Gerais, Brazil. J. Appl. Ichthyol. 19, 387–390.
Rose, N.R., 2002. Mechanisms of autoimmunity. Semin. Liver Dis. 22, 387–394.
Runnegar, M.T., Kong, S., Berndt, N., 1993. Protein phosphatase inhibition and *in vivo* hepatotoxicity of microcystins. Am. J. Physiol. 265, G224–G230.
Sant'Anna, C.L., Azevedo, M.T.P., Werner, V.R., Dogo, C.R., Rios, F.R., Carvalho, L.R., 2008. Review of toxic species of Cyanobacteria in Brazil. Algol. Stud. 126, 251–265.
Santos, A.P.M.E., Bracarense, A.P.F.R.L., 2008. Hepatotocidade associada à microcistina. Semin: Cien. Agrar. 29, 417–430.
Tencalla, F., Dietrich, D., 1997. Biochemical characterization of microcystin toxicity in rainbow trout (*Oncorhynchus mykiss*). Toxicon 35, 583–595.
Vieira, J.M.S., Azevedo, M.T.P., Azevedo, S.M.F.O., Honda, R.Y., Correa, B., 2003. Microcystin production by *Radiocystis fernandoi* (Chroococcales, cyanobacteria) isolated from a drinking water reservoir in the city of Belém, PA, Brazilian amazonia region. Toxicon 42, 709–713.
WHO – World Health Organization, 1998. Cyanobacterial toxins: microcystin-LR in drinking-water. In: Guidelines for Drinking-Water Quality. WHO, Geneva, pp. 18.
Wu, L., Wang, Q., Tao, M., Chen, J., Ma, Z., Xie, P., 2013. Preliminary study of the distribution and accumulation of GSH/Cys metabolites of hepatotoxic microcystins-RR in common carp from a lake with protracted cyanobacterial bloom (Lake Taihu, China). Bull. Environ. Contam. Toxicol. 90, 382–386.
Xie, L., Xie, P., Ozawa, K., Honma, T., Yokoyama, A., Park, H.-D., 2004. Dynamics of microcystins-LR and –RR in the phytoplanktivorous silver carp in a sub-chronic toxicity experiment. Environ. Pollut. 127, 431–439.
Xie, L., Yan, W., Li, J., Yu, L., Wang, J., Li, G., Chen, N., Steinman, A.D., 2015. Microcystin-RR exposure results in growth impairment by disrupting thyroid endocrine in zebrafish larvae. Aquat. Toxicol. 164, 16–22.
Zhang, W., Liang, G., Wu, L., Tuo, X., Wang, W., Chen, J., Xie, P., 2013. Why mammals more susceptible to the hepatotoxic microcystins than fish: evidences from plasma and albumin protein binding through equilibrium dialyses. Ecotoxicology 22, 1012–1019.